Marine Biotechnology (2022) 24:263–275
https://doi.org/10.1007/s10126-022-10098-z

ORIGINAL ARTICLE

Heme-Peroxidase 2 Modulated by POU2F1 and SOX5 is Involved in Pigmentation in Pacific Oyster (*Crassostrea gigas*)

Yue Min[1] · Qi Li[1,2] · Hong Yu[1]

Received: 10 November 2021 / Accepted: 30 January 2022 / Published online: 11 March 2022

Abstract

Color polymorphism is frequently observed in molluscan shellfish, while the molecular regulation of shell pigmentation is not well understood. Peroxidase is a key enzyme involved in melanogenesis. Here, we identified a heme-peroxidase 2 gene (*CgHPX2*), and characterized the expression patterns and transcriptional regulation of *CgHPX2* in the Pacific oyster *Crassostrea gigas*. Tissues expression analysis showed that *CgHPX2* was a mantle-specific gene and primarily expressed in the edge mantle in black shell color oyster compared with white shell oyster. In situ hybridization showed that strong signals for *CgHPX2* were detected in the both inner and outer surface of the outer fold of mantle in the black shell color oyster, whereas positive signals in white shell oyster were mainly localized in the outer surface of the outer fold of mantle. In the embryos and larvae, a high expression level of *CgHPX2* was detected in the trochophore stage in both black and white shell color oysters. The temporal localization of *CgHPX2* was mainly detected in the shell gland and edge mantle of trochophore and calcified shell larvae, respectively. In addition, a 2227 bp of 5′ flanking region sequence of *CgHPX2* was cloned, which contained a presumed core promoter region and many potential transcription factor binding sites. Further luciferase assay experiment confirmed that POU domain, class 2, transcription factor 1 (*POU2F1*), and SRY-box transcription factor 5 (*SOX5*) were involved in transcriptional regulation of *CgHPX2* gene through binding to its specific promoter region. After *CgPOU2F1* and *CgSOX5* RNA interference, the *CgHPX2* gene expression was significantly decreased. These results suggested that *CgPOU2F1* and *CgSOX5* might be two important transcription factors that positively regulated the expression of *CgHPX2* gene, improving our understanding of the transcriptional regulation of molluscan shell pigmentation.

Keywords *CgHPX2* · Transcriptional regulation · Melanin · Development

Introduction

Coloration is one of the most diverse and remarkable phenotypes in animals, with multiple functions including attraction, warning, camouflage, recognition, thermoregulation, and photoreception (Du et al. 2019; Parichy 2003). Significant advances have been made toward the characterization of pigments and their biosynthetic pathways for vertebrates and certain invertebrate groups (Fujiwara and Nishikawa 2016; Luo et al. 2021; Wittkopp and Beldade 2009). Mollusks are often renowned for their colorful shells, and have attracted the interest of the naturalists and biologists. However, molecular mechanism leading to shell pigmentation has not been fully uncovered in molluscan. Shell color is most commonly due to the presence of biological pigments. Three classes of biological pigments have been identified in molluscan shells including melanins, tetrapyrroles, and carotenoids (Williams 2017). Of them, melanin is the most widespread pigment in nature, which is made up of two classes: eumelanin which are black or brown, and pheomelanin which are red, orange, or yellow (Affenzeller et al. 2019).

Mollusk shells are produced by the outer fold of the mantle (Boettiger et al. 2009; Budd et al. 2014). Generally, shells grow in a linear fashion by adding new material to the growing edge which is in contact with the mantle tissues. Similarly, pigments are produced by the mantle and incorporated into the shell along the growing edge, the position

✉ Qi Li
qili66@ouc.edu.cn

[1] Key Laboratory of Mariculture (Ocean University of China), Ministry of Education College of Fisheries, Ocean University of China, Qingdao 266003, China

[2] Laboratory for Marine Fisheries Science and Food Production Processes, Qingdao National Laboratory for Marine Science and Technology, Qingdao 266237, China

of which continually changes over time as new shell is added (Fowler et al. 1992). It seems to have a relevant relationship between shell color and shell formation. For instance, in insects, cuticle tanning (pigmentation and sclerotization) is related to tyrosine metabolism, which is possessed of dual functions with darkening and hardening of cuticle (Noh et al. 2016). In molluscan, some conserved enzymes involved in melanogenesis might participate in periostracum formation by cross-linking fibrous proteins rich in reactive quinones to form water-insoluble, protease-resistant polymers (Feng et al. 2019; Herlitze et al. 2018; Zhu et al. 2021).

Recently, a large amount of omics data has been generated in mollusca related to shell pigmentation (Hu et al. 2020; Huang et al. 2021; Nie et al. 2020; Xu et al. 2019a, b). Although some potential genes that may participate in shell pigmentation have been identified, it is not possible to rule out which may be involved in biomineralization. In *Pinctada margaritifera*, comparative transcriptome analysis suggested that the nacre color was influenced by the genes involved in the biomineralization of the calcitic layer (Lemer et al. 2015). In *Patinopecten yessoensis*, several dual functioning proteins were identified in both biomineralization and melanogenesis including calmodulin and related proteins and Ca^{2+}/calmodulin-dependent protein kinase (Sun et al. 2015). Additionally, other notable proteins, tyrosinase and tyrosinase-like protein, played similar functions in *Crassostrea gigas* (Zhu et al. 2021). Peroxidase was identified at the mantle zone of belt and groove in *Lymnaea stagnalis*, indicating that peroxidase played a key role in periostracum formation (Timmermans 1968). Further researches demonstrated that mantle peroxidase was specifically expressed in mantle lobes, an embryonic shell marker (Shimizu et al. 2017). In addition, peroxidase activity was applied as a marker to map molluscan shell development (Hohagen and Jackson 2013; Johnson et al. 2019). In cephalopod, peroxidases are associated with melanosomes in the ink gland (Charles 2014), which is indicated that *peroxidase* plays vital roles in melanogenesis of mollusca. In *C. gigas*, *peroxidase* genes have suffered from expansion and nine out of 26 *peroxidase* genes are highly expressed in the mantle (Feng et al. 2017). It has been suggested that *peroxidase* plays various roles involving biomineralization and melanogenesis.

The Pacific oyster *C. gigas* is a widely distributed and most productive economically species in the world. Shell color is regarded as an economic trait in many breeding programs of mollusks. Four shell color strains (golden, white, black, and orange) of *C. gigas* were successfully developed (Ge et al. 2015; Han and Li 2020; Xu et al. 2019a). Integrated analysis of microRNA and mRNA expression profiles in *C. gigas* revealed that lgi-miR-317 and its targets peroxidase and lncRNATCONS_00951105 acting as the competing endogenous RNA to regulate melanogenesis (Feng et al. 2020). Additionally, knockdown of heme-peroxidase 2 gene (*CgHPX2*) could block melanogenesis in the adult Pacific oysters, indicating that peroxidase plays a vital role in the shell pigmentation (Feng et al. 2019). However, the information on the function and transcriptional regulation of *CgHPX2* is limited.

In the present study, *CgHPX2* was identified and characterized in *C. gigas*. Expression profiles in different embryo-larval developmental stages and different tissues were detected. In addition, we analyzed *CgHPX2* promoter and investigated the transcriptional regulation of *CgHPX2*. Our results provided the foundation for understanding the transcriptional regulation of *CgHPX2* and shedding light on the mechanism of melanogenesis.

Materials and Methods

Sample Collection

One-year-old Pacific oysters were collected from Weihai, Shandong, China, which were divided into two groups, including one black experiment group and one white shell control group. The mantle was fixed in 4% paraformaldehyde at 4 °C overnight for tissues in situ hybridization (ISH). Six tissues including edge mantle, central mantle, adductor, gills, labial palp, and digestive gland were dissected, flash-frozen in liquid nitrogen, and stored at −80 °C freezer until RNA isolation. Samples of each tissue collected from nine individuals were pooled into three biological replicates (three individuals/replicate).

Embryonic and larval samples were obtained from black and white shell color strains in Laizhou, Shandong, China, at the following stages: fertilized egg, multi-cells, blastula, gastrula, trochophore, early D-shaped larvae, late D-shaped larvae, Umbo larvae, and eyed larvae stages. The detailed sampling time can be seen in Table S1. Larval samples were treated and stored the same as adult tissues procedure.

RNA Extraction and Real-Time qPCR

Total RNA was extracted using RNAeasy animal RNA extraction kit (Beyotime, China) according to the manufacturer's instructions. The quality and concentration of RNA were detected by Nanodrop 2000 (Thermo, USA) and analyzed in a 1.5% agarose gel electrophoresis. The total RNA was reverse transcripted into cDNA by HiScript III 1st strand cDNA synthesis kit (Vazyme, China).

The real-time PCRs were amplified by using QuantiNova SYBR Green PCR kit (Qiagen, Germany) on a Lightcycler 480 real-time PCR instrument (Roche, Switzerland). The specific primers were designed using Primer Premier 5.0 software (Premier Biosoft International, Palo Alto, CA) (Table S2), and its availability was detected by conventional

PCR and melting curve analysis. Elongation factor 1-α (*ef1α*) was internal control in adult samples (Li et al. 2021). In larvae, elongation factor 1-α (*ef1α*), adp-ribosylation factor 1 (*arf1*), and glyceraldehyde-3 phosphate-dehydrogenase (*gaph*) were used as internal references for normalization (Huan et al. 2016). The relative expression was calculated by the $2^{-\Delta\Delta CT}$ method. All the data and significant differences were analyzed using GraphPad Prism 8.0 by one-way ANOVA and two-way ANOVA followed by single or multiple comparisons. Differences were considered statistically significant at $P < 0.05$.

Identifying and Cloning the Coding Sequence of *CgHPX2*

The *CgHPX2* coding sequence was amplified by PCR based on sequence information downloaded from the National Centre for Biotechnology Information (NCBI, https://www.ncbi.nlm.nih.gov; accession: LOC105324712). The specific primer sequences used in amplification are listed in Table S2. The PCR was performed using Phanta Max super-Fidelity DNA polymerase (Vazyme, China) according to the manufacturer's protocols. PCR products were detected by 1.5% agarose gel electrophoresis.

Bioinformatics Analysis of *CgHPX2*

The isoelectric point (pI) and molecular weight (MW) of deduced amino acid sequences were predicted using the Compute pI/MW Tool at the ExPAsy site (http://web.expasy.org/compute_pi/). The conserved domains of *CgHPX2* were predicted from the CD-Search tool of NCBI (https://www.ncbi.nlm.nih.gov/Structure/cdd/wrpsb.cgi). The secondary and the tertiary structure were predicted by Phyre2 (http://www.sbg.bio.ic.ac.uk/~phyre2/html/page.cgi?id=index). The amino acid sequences alignment was performed using the ClustalW (Lynnon Biosoft, Los Angeles, CA) program and modified by ESPrint 3.0 (Xavier and Patrice 2014). The phylogenetic trees were performed on MEGA 7.0 (Kumar et al. 2016) using the maximum likelihood (ML) methods with 1000 bootstrap replicates.

RNA Location Pattern Analysis of *CgHPX2* by in Situ Hybridization

Tissues in situ hybridization (TISH) and whole mount in situ hybridization (WISH) were used to analyze RNA location patterns in adult tissues and different developmental larvae, respectively. To synthesize specific RNA probes, specific cDNA fragments were amplified with primers in Table S2 which were tagged with a T7 promoter sequence (GAT CACTAATACGACTCACTATAGGG). The PCR products were purified using DNA purification kit (Thermo, USA). The purified PCR products were used as the template for T7-mediated in vitro transcription by DIG-RNA labeling kit (Roche, Switzerland). The TISH was performed with 5-μm thick sections after the preparation of probes. After a series of deparaffinization, prehybridization, hybridization, and antibody incubation, the section was incubated in 2% NBT/BCIP solution (Roche, Switzerland) for 1 h at room temperature or at 4 °C overnight. When specific signal was detected, the 0.5% eosin was used to re-stain the slides. For WISH, the embryos were treated by proteinase K (Solarbio, China) with an age-dependent concentration (Hohagen et al. 2015). The detailed procedure was performed as described previously (Li et al. 2021; Yue et al. 2021). All the TISH and WISH images were taken with an Olympus BX53 microscope coupled with a DP80 camera (Olympus, Japan).

Luciferase Vector Construction and Site-Directed Mutagenesis

To identify the core promoter region, different length 5′ flanking sequences of *CgHPX2* were subcloned into pGL3-Basic vector (Promega, USA) using ClonExpress II One Step Cloning Kit (Vazyme, China). Six 5′ deletion constructs (P1: − 2011 ~ + 216, P2: − 1726 ~ + 216, P3: − 1519 ~ + 216, P4: − 1221 ~ + 216, P5: − 453 ~ + 216, P6: − 351 ~ + 216) from the start codon of *CgHPX2* were generated using *C. gigas* genomic DNA as a template. In addition, primers containing the homologous sequence of the expression plasmids pcDNA3.1 vector (Promega, USA) were used to amplify the CDS of *CgPOU2F1* and *CgSOX5* and then subcloned into pcDNA3.1 vector. The site-directed mutagenesis constructs were produced according to the manufacturer's instructions of Mut Express MultiS Fast Mutagenesis kit V2 (Vazyme, China). All the plasmids constructed were verified by sequencing analysis and the primer sequences used in this study are provided in Table S2.

Cell Culture, Transient Transfections, and Dual-Luciferase Reporter Assays

HEK-293T cells were cultured in DMEM (Solarbio, China) supplemented with 10% fetal bovine serum (Hyclone, USA) and 1% 1X penicillin–streptomycin antibiotics solution (Hyclone, USA) at 37 °C with 5% CO_2. The cells were then plated into 24-well plates (CORNING, USA) and grown under the confluence of 70–90% cells. Cells were transfected using lipofectamine 3000 (Invitrogen, CA, USA) in accordance with the manufacturer's instructions. The pRL-TK plasmid (Progema, USA) was co-transfected with cells as internal control to normalize transfection efficiency. For simple transfection, six 500 ng promoter truncation recombination vectors were co-transfected with 10 ng pRL-TK plasmid into 24-well cells, respectively. For co-transfection with

CgPOU2F1 or *CgSOX5*, 250 ng of recombinant pcDNA3.1 expression vector, 250 ng of recombinant pGL3-Basic vector, and 5 ng pRL-TK plasmid were used for each well of a 24-well plate. Luciferase reporter analysis was performed 48 h after transfection. After removal of medium, cells were quickly washed with DPBS (Solarbio, China) and then lysed using luciferase lysis buffer (Progema, USA). Firefly and Renilla luciferase activities were measured by the dual-luciferase reporter assay system (Progema, USA) at the manufacturer's protocol and chemiluminescence were read using Synergy™ H1 (BioTek, USA). The relative luciferase activity (Firefly luciferase activity: Renilla luciferase activity) was analyzed by one-way ANOVA using GraphPad Prism 8.0.

Subcellular Localization of POU2F1 and SOX5

The coding sequence of *CgPOU2F1* and *CgSOX5* was subcloned into the expression vector pEGFP-1 (www.miaolingbio.com) for expression of GFP fusion protein. The HEK-293T cells plated into the confocal dish (Lecia, USA) were transfected with CgPOU2F1-pEGFP-1 or CgSOX5-pEGFP-1 recombinant expression vectors. After incubation for 48 h, the cells were stained with 4′,6-diamidino-2-phenylindole (DAPI) (Beyotime, China) for 25 min in darkness. The image acquisition and analysis were performed on an ultra-high-resolution laser confocal microscope Lecia TCS SP8 STED 3X equipped with Lecia Application Suite X software. Primers used for fusion vector construction are listed in Table S2.

RNA Interference Experiment

In vivo RNAi experiments, feeding dsRNA-expressing bacteria to study shell pigmentation which was previously reported in adult oysters (Feng et al. 2019). During the interference phase, each group with three tanks of black shell color strain of Umbo larvae (> 200 μm) was continuously exposed to the algae/dsRNA-producing bacteria to co-inoculum. Three dsRNA-producing bacteria were prepared by including *E. coli* strain HT115 (DE3) bacteria transformed with three constructed plasmids (*CgPOU2F1*-L4440, *CgSOX5*-L4440, *EGFP*-L4440) with isopropylβ-D-thiogalactoside (IPTG). The *EGFP*-L4440 was previously constructed in the laboratory. Algae/bacteria co-inoculum was produced by mixing algal culture and bacterial suspension at a ratio of 100 bacteria per algal cell with a final *Platymonas subcordiformis* concentration of 25, 000 cells ml^{-1}. Food reserves were renewed with fresh algae/bacteria co-inoculum. After recombinant plasmids were induced with IPTG, plasmids were centrifuged and resuspended in 500 ml *P. subcordiformis* algae culture liquid. Larvae specimens were sampled at day 7 and day 14, respectively. With regard to recombinant plasmid constructions, expression of dsRNA and related qPCR primers is shown in Table S2.

Results

Bioinformatics, Homology, and Phylogenetic Analysis of *CgHPX2*

A single *CgHPX2* gene was identified from the *C. gigas* genome database. The basic information of *CgHPX2* is summarized in Table S3. The complete DNA sequence of *CgHPX2* was 11,219 bp containing 12 exons and 11 introns. The intron–exon boundaries were distinguished by the GT-AG rule. The full length cDNA of *CgHPX2* was 3301 bp with 101 bp 5′ UTR, 566 bp 3′ UTR, and 2634 bp ORF encoding 877 amino acids. The predicted molecular weight of *CgHPX2* was 98.77 kDa with an isoelectric point (pI) of 9.49. The putative protein secondary structure consisted of 44% alpha helixes and 3% beta strands (Fig. 1A). The tertiary structure of HPX2 protein was based on template c2gjmA, which shared 33% identity with *CgHPX2* protein (Fig. 1B).

The homology between *CgHPX2* and deduced amino acid sequences of other species was explored via multiple sequence alignment. Sequences were available on GenBank (*Crassostrea virginica*, XP_022291683.1; *Pecten maximus*, XP_033758659.1; *Mizuhopecten yessoensis*, XP_021358145.1; *Lingula anatina*, XP_013419078.1; *Octopus vulgaris*, XP_029656077.1; *Amphibalanus amphitrite*, KAF0313953.1; *Bemisia tabaci*, XP_018902871.1; *Daphnia magna*, XP_032798431.1; *Rhopalosiphum maidis*, XP_026811832.1). Sequence alignment of *CgHPX2* with peroxidase protein from other species showed a moderate degree of sequence similarity and possessed an animal haem peroxidase domain (Fig. S5).

Phylogenetic analysis was performed to investigate the relationship between *CgHPX2* and other family members. Their gene names and accession numbers are provided in Table S4. Phylogenetic analysis showed that *CgHPX2* were clustered with cephalopoda homologs (99% similarity), and all the mollusca species were clustered together (Fig. 1C). The peroxidase-related protein formed two major groups. Pacific oyster HPX2 protein, together with other mollusca, formed a major group distinct from vertebrate homologs.

Expression Profiles of *CgHPX2*

To investigate the role of the *CgHPX2* gene in the shell color, the expression level of *CgHPX2* was first analyzed

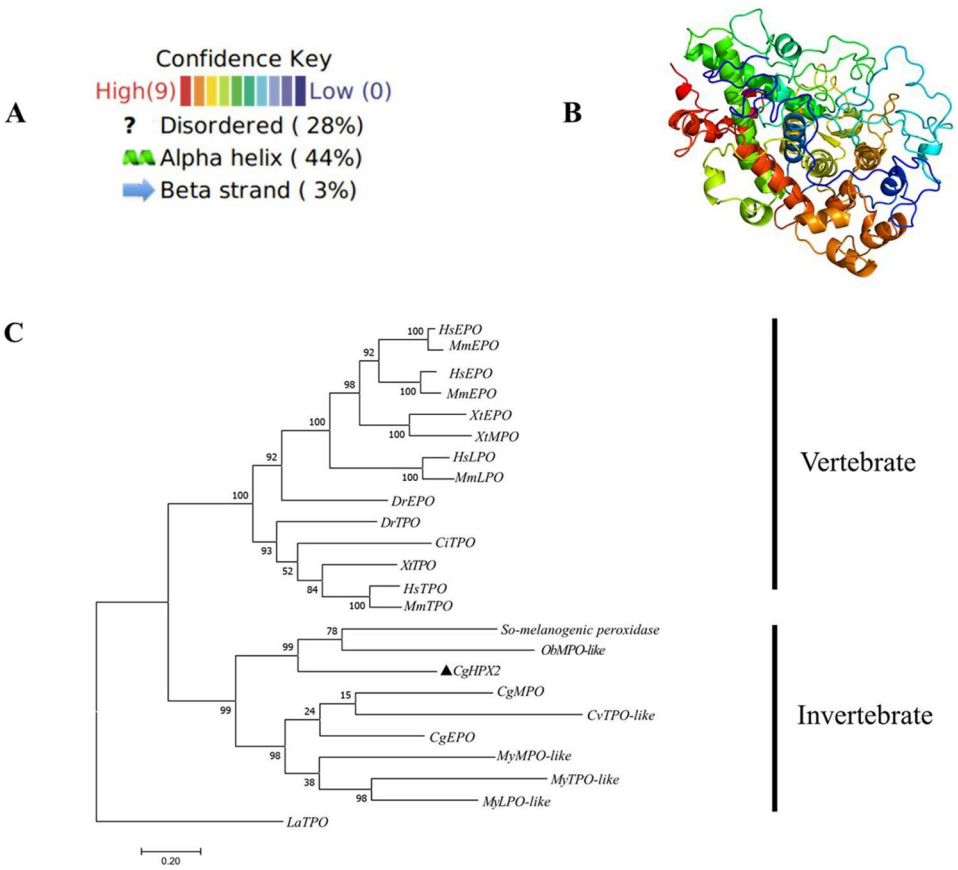

Fig. 1 The spatial structure of *CgHPX2* and phylogenetic tree of the *CgHPX2*. **A** The predicted secondary structure of the *CgHPX2* protein. The putative secondary structure of CgHPX2 contained 44% alpha helices and 3% beta strand structures; **B** the predicted tertiary structure of the *CgHPX2* protein; **C** molecular phylogenetic tree of *CgHPX2* constructed by the maximum likelihood (ML) method. The numbers at the nodes indicate the bootstrap proportions after 1000 replicates

in different tissues and different developmental stages. Higher expression was observed in the edge mantle and central mantle, while the lower mRNA levels were observed in the digestive gland, adductor muscle, gill, and labial palps ($P < 0.05$) (Fig. 2A). The expression of *CgHPX2* in the edge mantle of black shell strains was

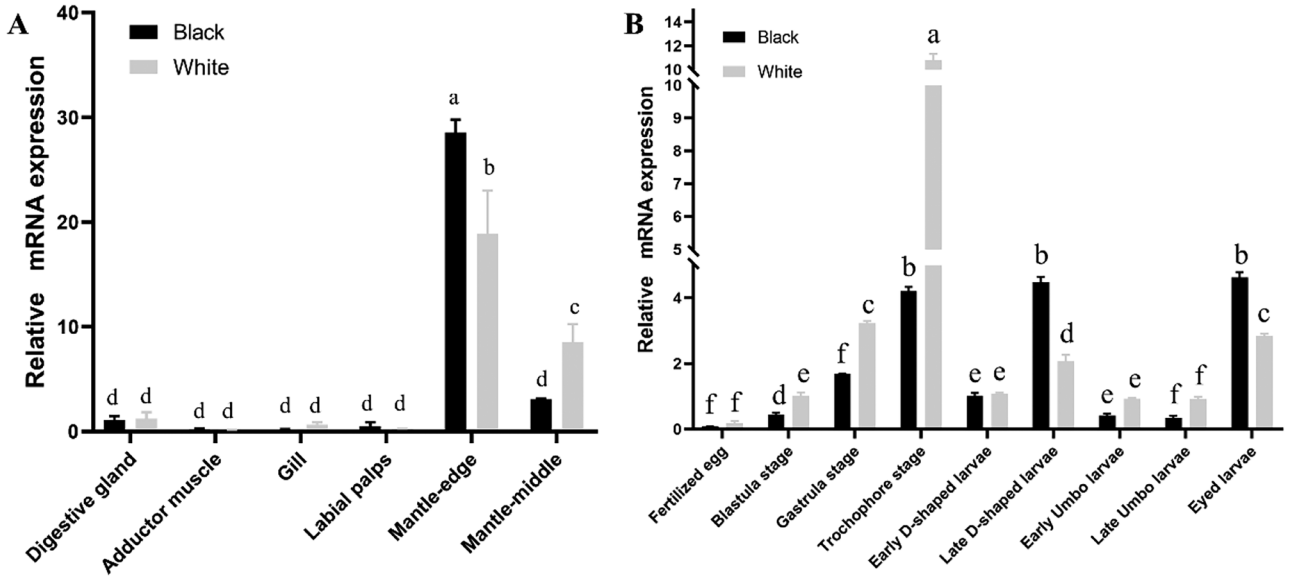

Fig. 2 The mRNA expression profiles of *CgHPX2*. **A** Expression patterns of *CgHPX2* in different adult tissues in black and white shell color strains. **B** Expression profiles of *CgHPX2* during embryo-larval developmental stages in black and white shell color strains. Different letters indicated significant difference ($P < 0.05$)

significantly higher than in white shell strains. Moreover, the localization of specific signal in different shell color mantles (black and white) was abundantly in the outer mantle fold (Fig. 3). In the outer mantle fold, the specific signal was detected in the columnar epithelium. In addition, the specific signal intensity and coverage in black shell were significantly stronger than white shell.

During the embryo-larval development, *CgHPX2* mRNA expression profiles were similar among different shell color strains (black and white) (Fig. 2B). The expression of *CgHPX2* increased sharply from blastula stage, peaking at trochophore stage, in which the expression level of *CgHPX2* was significantly higher in white shell strains than in black ($P < 0.05$). After trochophore stage, the expression of *CgHPX2* dramatically fluctuated. Furthermore, the spatial patterns of *CgHPX2* mRNA expression were analyzed by WISH from fertilized egg to eyed larvae (Fig. 4). The positive signal localization pattern was similar in both black and white shell larvae. In black shell larvae, the positive signal was detected in the trochophore stage as cell cluster (Fig. 4-I-E). In D-shaped larvae, Umbo larvae, and eyed larvae, the specific staining formed a regular pattern and the positive signals were all detected in the edge of the larval mantle (Fig. 4-I). Compared with white shell larvae (Fig. 4-II), the staining with antisense probes is noticeably stronger, except for trochophore stage, which is consistent with the real-time PCR results.

The Sequence Analysis of the 5′-Upstream Regulatory Region of *CgHPX2* Gene

The 2227 bp 5′ flanking fragment was cloned according to the *C. gigas* genome database. Promoter sequence analysis showed that the transcription start site is located at −216 bp upstream of the start codon ATG, and the nearest TATA box is located at −730 bp. Potential transcription factor binding sites include *POU2F1*, *SOX5*, microphthalmia-associated transcription factor (*MITF*), cAMP response element binding protein (*CREB*), *GATA-3*, and so on (Fig. 5A). These cis-acting elements may be crucial for the transcriptional regulation of *CgHPX2* gene.

Identification of the Core Region of the *CgHPX2* Promoter and Key Transcription Factor

To detect the transcriptional activities of the promoter region, six truncation fragments of 5′ flanking sequence with different lengths were subcloned into pGL3-basic vector and then transiently transfected into HEK-293 T cells. The dual-luciferase reporter system results showed that the transcriptional activity was significantly decreased with the deletion of *CgHPX2* 5′ flanking sequence (Fig. 5B). The transcriptional activity of *CgHPX2* was significantly decreased by 65.69% after deletion of −1519 ~ −1221 fragment. Compared with P4 (−1221/+214), the other deletion

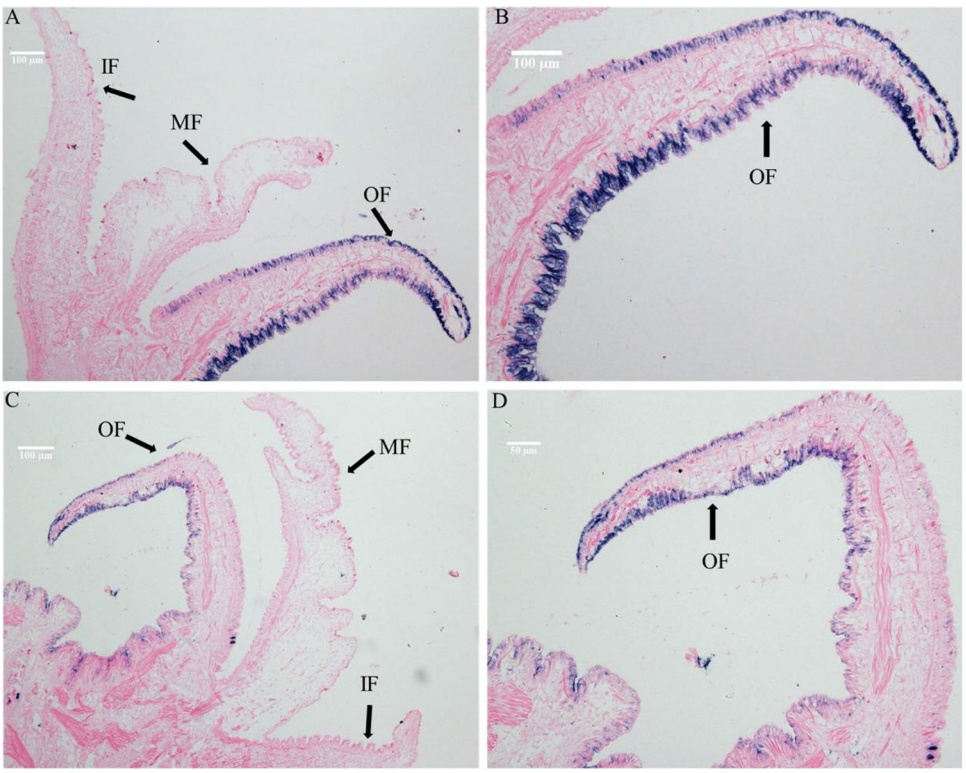

Fig. 3 The mRNA localization of *CgHPX2* in adult mantles. **A** and **B**, **C** and **D** represent black shell strains white shell strains, respectively. OF, outer fold of mantle; MF, middle fold of mantle; IF, inner fold of mantle

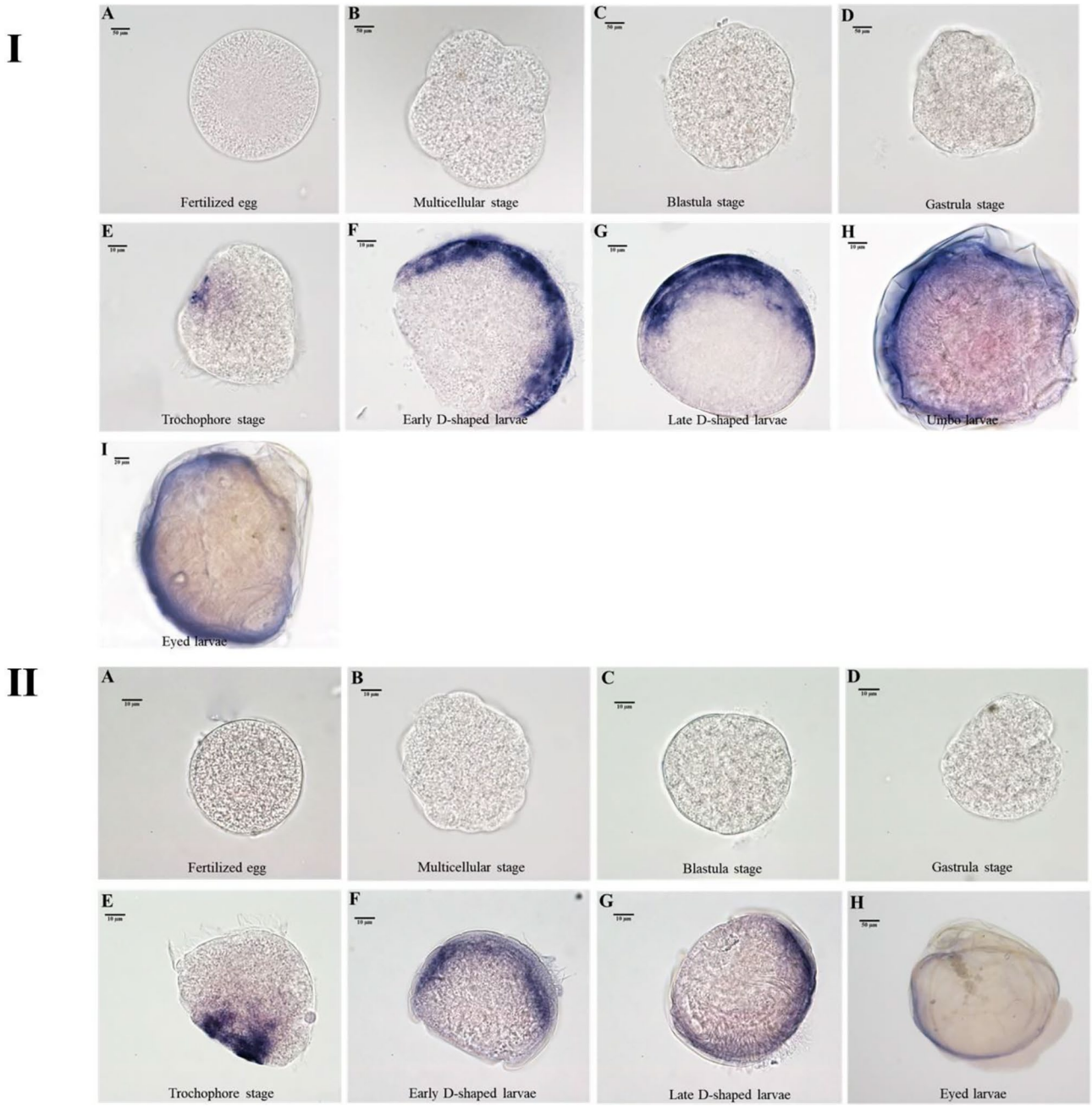

Fig. 4 The spatial pattern of *CgHPX2* mRNA localization in embryonic and larval developmental stages. **I** and **II** represent black and white shell color strains, respectively

of promoter fragments showed no difference in transcriptional activity, which indicated that the core promoter regulatory region is located between −1519 and −1221 bp upstream of *CgHPX2*.

Two transcription factor binding sites were identified in the core promoter region. To further explore whether *CgPOU2F1* and *CgSOX5* participate in the transcriptional regulation of *CgHPX2*, co-transfection studies followed by dual-luciferase assays experiments were performed. As shown in Fig. 5C, D, mutation of *CgPOU2F1* and *CgSOX5* binding sites and the enzyme activity of mut-POU2F1 and mut-SOX5 groups were significantly lower than the non-mutated group. Taken together, these results showed that the presence of *POU2F1* and *SOX5* transcription factors can improve the transcriptional activity of the *HPX2* gene.

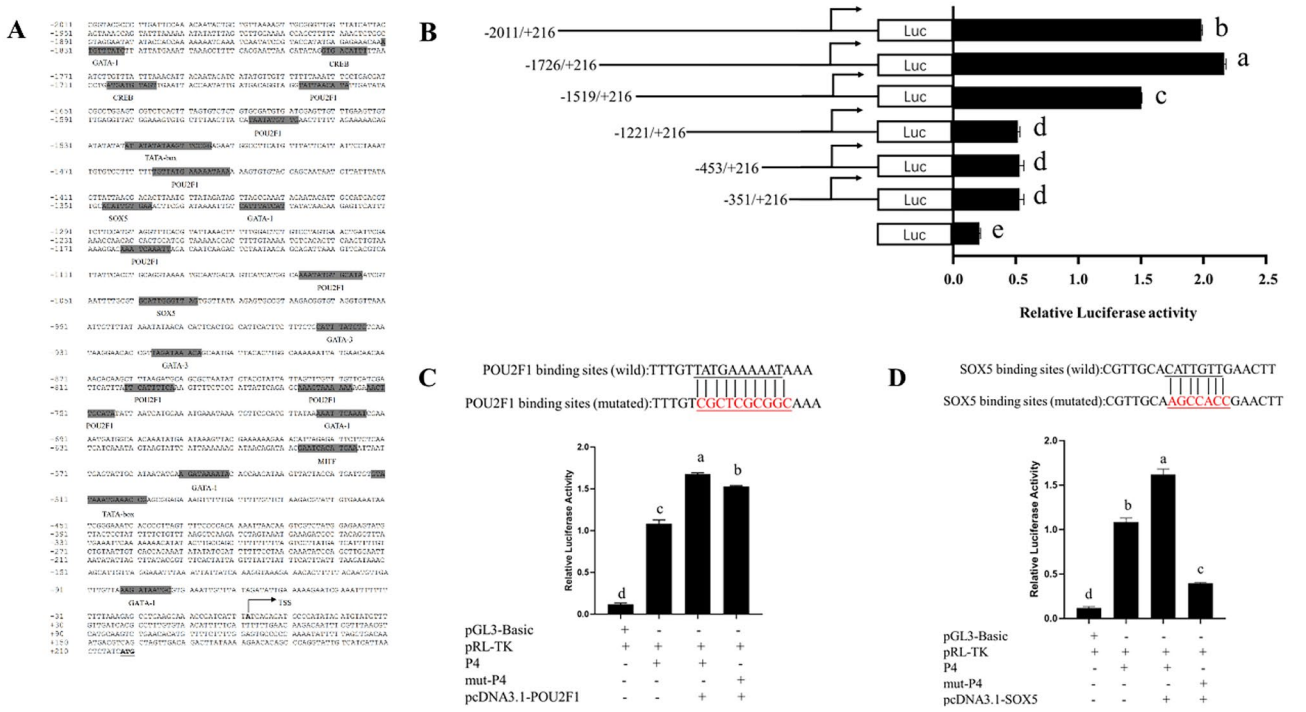

Fig. 5 Results of putative cis-acting elements prediction and point mutation enzyme activity measurement in *CgHPX2* promoter region. **A** Results of cis-acting elements prediction in the 5′ flanking region. **B** Identification of the core transcriptional regulatory region at −1519 ~ −1221. **C** and **D** Enzyme activity measurement of point mutation of transcription factor POU2F1 and SOX5; pGL3-basic represents empty carrier group; pRL-TK represents internal control group; P4 represents core promoter region group; mut-P4 represents mutation of transcription factor POU2F1 or SOX5 binding sites; pcDNA3.1-POU2F1 and pcDNA3.1-SOX5 represent the combination protein vectors. "+" and "−" indicate that the plasmid was transfected into the HEK-293 T or not. Different letters indicated significant difference $P < 0.05$

CgPOU2F1 and CgSOX5 are Located in the Nucleus in HEK-293 T Cells

To reveal the subcellular localization of two transcription factors, a green fluorescent protein (GFP)-tagged CgPOU2F1 and CgSOX5 were transfected into HEK-293 T cells. In CgPOU2F1-pEGFP- and CgSOX5-pEGFP-transfected cells, the GFP signals merged with the DAPI signals (Fig. 6). These results implied that *CgPOU2F1* and *CgSOX5* are localized in the nucleus of HEK-293T cells, consistent with their roles as transcription factors.

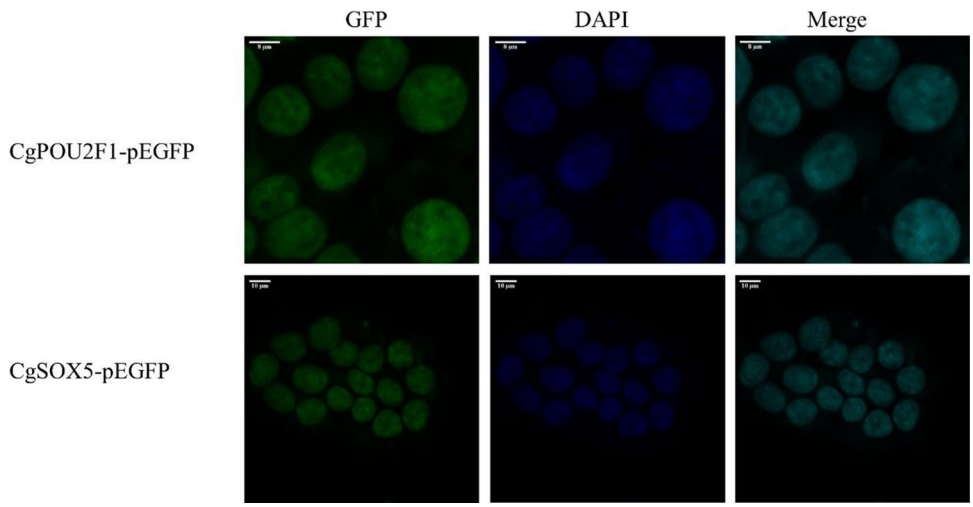

Fig. 6 Subcellular localization of *CgPOU2F1* and *CgSOX5* in HEK-293 T cells. HEK-293 T cells were transfected with EGFP reporter constructs expression an EGFP-tagged POU2F1 and SOX5, respectively. Nuclear DNA was stained with DAPI and cells were analyzed with a fluorescence confocal microscope

CgPOU2F1 and *CgSOX5* Knockdown Led to a Decrease in *CgHPX2* Expression

To further clarify the function of the *CgPOU2F1* and *CgSOX5* in the regulation of *CgHPX2*, *CgPOU2F1* and *CgSOX5* knockdown in vivo using dsRNA was performed. The expression of dsRNAs was induced in *E. coli* strains which were incubated with 0.4 mM IPTG at 37 °C for 4 h. Bands of dsRNA corresponding to *POU2F1* and *SOX5* genes sequence between two T7 promoters were observed in the IPTG-induced *E. coli* (Fig. S6), indicating the corresponding expression of dsRNA in *E. coli*.

To detect target gene expression level, qPCR results showed that the expression level of bacteria-expressing *CgPOU2F1* and *CgSOX5* dsRNA was significantly dropped as compared to the control group in day 7 and day 14, respectively (Fig. S7).

Compared with the group fed with EGFP dsRNA-expressing bacteria, the expression level of downstream gene *CgHPX2* was significantly decreased in RNAi-treated group (Fig. 7). In POU2F1 dsRNA-expressing bacteria-treated group, the expression level of *CgHPX2* was significantly decreased by 69% and 88% compared with the negative control group on day 7 and day 14, respectively. In *SOX5* dsRNA-expressing bacteria-treated group, *CgHPX2* mRNA expression level dropped down to 57% on day 14.

Discussion

Heme-peroxidase 2 is a member of the peroxidase superfamily, possessed a conserved animal haem peroxidase domain. The prosthetic heme group is a derivative of protoporphyrin IX, which is an essential component of the catalytic scheme in heme peroxidases (Singh et al. 2017). Heme peroxidases are readily abundant enzymes that can be classified into two major families, namely animal and non-animal peroxidases (Loughran et al. 2008). *CgHPX2* belongs to the category of animal peroxidases that includes mammalian myeloperoxidase (*MPO*), lactoperoxidase (*LPO*), eosinophil peroxidase (*EPO*), and thyroid peroxidase (*TPO*) (Loughran et al. 2008). Phylogenetic analysis of *CgHPX2* protein with peroxidases from other species revealed that *CgHPX2* was clustered with cephalopoda melanogenic peroxidase (99% similarity), which indicated that the two peroxidases possibly shared similar function. In *Sepia officinalis*, melanogenic peroxidase was the last enzyme involved in eumelanin synthesis in ink gland (Charles 2014). This implied that *CgHPX2* possibly possessed the ability of eumelanin synthesis, which was consistent with the previous RNAi experiment (Feng et al. 2019).

Peroxidase genes played a critical role in various physiological processes, including melanin synthesis, shell formation, and wing maturation (Charles 2014; Dondra et al. 2017; Timmermans 1968). In this study, temporal expression analysis revealed that *CgHPX2* was more highly expressed in the trochophore stage larvae of white shell color strains than black shell color strains, which indicated that *CgHPX2* played different roles in white and black shell color larvae, including shell biomineralization and pigmentation. Firstly, the white shell color is a kind of albino phenotype, which might overcompensate for non-functional melanin protein by overexpressing the gene for this protein in larval stage and therefore might have difficulty in incorporating pigments into organic matrix. In terms of coloration, although most larvae appear unpigmented, pigments may contribute to color in later shell or the content of pigment is too low to be detected. Secondly, the trochophore stage is a crucial stage for larval shell formation. The expression of *CgHPX2* reached the peak

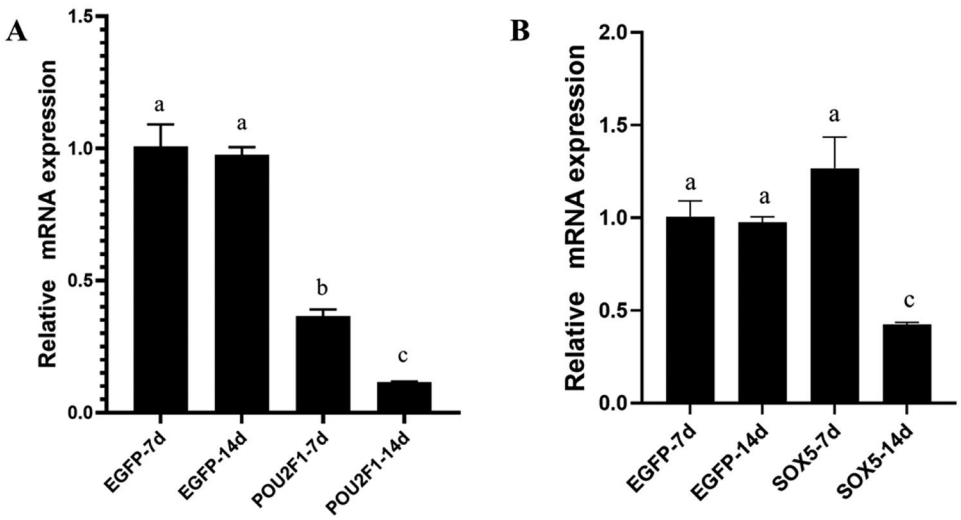

Fig. 7 RNAi knockdown of the *CgPOU2F1* and *CgSOX5* gene. **A** The relative expression levels of *CgHPX2* in the Umbo larvae stage after ingested with dsPOU2F1 and dsEGFP. **B** The relative expression levels of *CgHPX2* in the Umbo larvae stage after ingested with dsEGFP and dsSOX5. The data are expressed as mean ± SD ($n = 3$). Different letters indicated significant differences, $P < 0.05$

in the trochophore stage in both white shell color strains and black shell color strains. The development of the shell can be divided into five stages (Kin et al. 2009). The shell begins to form prodissoconch I during the trochophore stage, followed by prodissoconch II in D-shaped larval stage (Kin et al. 2009). Therefore, larval shell formation is an important biological event in trochophore stage, which suggested that *CgHPX2* played important role in larval shell formation. Furthermore, studies have shown that there is a higher ratio of aragonite to pigments in regions with larger surface in *Mercenaria mercenaria* during trochophore and D-veliger stage, such as the prodissoconch I region (Thompson et al. 2014). Therefore, it is possible that pigment can occur from the prodissoconch I region and precise technology can be taken advantage of to detect pigment. Further studies using transmission electron microscopy, micro-Raman spectroscopy, and LC–MS are necessary to illustrate the origin of pigment.

The temporal expression patterns of the *CgHPX2* gene investigated in larvae of black and white shell color strains revealed a complexity to coordinate the deposition of larval shell and pigmentation formation. Importantly, larval shell-forming cells are thought to give rise to the fully differentiated adult shell-forming organ, the mantle, suggesting that trochophore, veliger, and adult shells do not have independent evolutionary origins as previously suggested (Gerhard et al. 1995). Moreover, recent studies revealed an interesting link between trochophore and adult mantle in regard to their remarkable usage of novel genes and the rapid evolution of the trochophore transcriptome potentially contributing to adult organ evolution (Wang et al. 2020). What's more, in the abalone *Haliotis asinina*, veliger mantle cells expressing shell-forming genes to do so following metamorphosis (Jackson et al. 2005, 2007). Therefore, trochophore is an important central stage in the larvae life cycle. Our study demonstrated that the positive signal was first detected in the shell gland in trochophore stage and then it was localized at the edge mantle, indicating *CgHPX2* participated in the larval shell formation.

Underlying the vast phenotype diversity of molluscan shells is an evolutionary homologous organ—the mantle—which directly contacts with the shell, producing shell pigments (Williams 2017). In *H. asinina*, pigments were localized in the edge mantle, indicating the important role of edge mantle region in shell pigmentation (Budd et al. 2014); however, the central mantle involved in shell pigmentation is still unclear. Tissue-specific expression revealed that *CgHPX2* was a mantle-specific gene. The expression level of *CgHPX2* in the edge mantle was much higher ($P < 0.05$) than that in the central mantle. The expression level of *CgHPX2* in the edge mantle of black shell strains was significantly higher ($P < 0.05$) than in white shell strains, proving that the edge mantle was involved in shell pigmentation.

Previous descriptions of the mantle margin morphogenesis in *Nodipecten nodosus* provided new insights into the roles of bivalve pallial folds (Audino et al. 2015). In Bivalvia, the mantle margin is divided into three pallial folds, each with a specific function: the secretory outer fold, the sensory middle fold, and the muscular inner fold (Audino et al. 2015). The periostracum is formed in a deep groove between the outer and middle folds, while the shell layers are secreted by the outer mantle epithelium. In addition, pigments can be found in the periostracum (Grant and Williams 2018). In this study, the specific signal of *CgHPX2* was located in the outer fold of the mantle, which was significantly higher in black shell color strains mantle than that in white shell color strains. Moreover, the histology and ultrastructure of mantle tissue in black and white shell color strains revealed the existence of melanocyte in both shell color strains (unpublished), which indicated that the white shell color strains were with the capacity to synthesize melanin and were likely to be defective in melanin transportation. Melanosomes are organelles which are responsible for the synthesis, storage, and transport of melanin (Tian et al. 2021). The mechanism of melanosomes transport is including membrane transport and cytoskeleton-dependent melanosomes transport (Rogers and Gelfand 2000; Granger et al. 2014). Studies have shown that Rab27a-melanophilin-Myo5a, a tripartite protein complex, regulates actin-based melanosomes transport (Ohbayashi and Fukuda 2020). In Oujiang color common carp, mutants with melanophilin (Rab effector proteins) mutation have caused large area black spot fading which is consistent with the black discoloration level (Hu et al. 2021). Moreover, it is reported that *Rab7* is associated with melanosome biogenesis and the transport of *TYRP1* from the trans-Golgi network to melanosome (Hirosaki et al. 2002). Similarly, we can hypothesize that the white shell color strains can synthesize melanin, but there are some transporter proteins responsible for transportation of pigment-related substrate to influence pigmentation in oyster. These results potentially revealed that *CgHPX2* was not only involved in the shell formation but also related to shell pigmentation.

Transcriptional regulation is a fundamental physiological process in organisms. Since most animals share a conserved repertoire of body-building and body-patterning genes, the complex expression patterns of developmentally regulated genes are typically controlled by numerous independent cis-regulatory elements (Prud'homme et al. 2007). A series of binding sites of melanocyte-related transcription factors within the 2227 bp 5′ flanking regions of *CgHPX2* were screened, including *CREB*, *SOX5*, *POU2F1*, *MITF*, and TATA box. All of these putative binding sites are pivotal for regulation of melanocytic survival in some vertebrate species. In zebrafish, for instance, *MITF:GFP* transgenic

accurately marked melanoblasts (Curran et al. 2009). *CREB* is a basic leucine zipper transcription factor, which is involved in nacre color formation in *Hyriopsis cumingii* (Zhang et al. 2021).

Melanin biosynthesis is a complex process, regulated by a number of signaling system and transcription factors. In mollusca, it is reported that several genes are involved in the biochemical pathway of melanogenesis and its regulation includes *MITF* (Mao et al. 2019; Zhang et al. 2018), paired box gene 3 (*PAX3*) (Yu et al. 2018), tyrosinase (*TYR*), and tyrosinase-related protein 1 and 2 (*TYRP1* and *TYRP2*) (Zhu et al. 2021). In the present study, two transcription factors, *CgPOU2F1* and *CgSOX5*, were identified. POU2F1, also known as Oct1 or OTF-1 (Besch and Berking 2014), belongs to POU class II, and is a potent regulator of stress responses, metabolism, tumorigenicity, phosphorylation, ubiquitination, O-GlcNAcylation, and other mechanism (Kang et al. 2013). Recent studies reported that POU2F1 negatively regulated the activity of solute carrier family 7 member 11 (*Slc7a11*) promoter, related to pheomelanin synthesis (Chen et al. 2019). Another transcription factor *CgSOX5* belongs to SOXD subgroup in SOX family (Yu et al. 2017). *SOX5* acted as fate switch in pigment cell lineages, and its function in xanthophores specification differs between different fish (Debbache and Sommer 2014; Nagao et al. 2018, 2014). Moreover, further research revealed that miR-21a-5p regulated melanogenesis via *MITF* by targeting *SOX5* (Wang et al. 2016). In this study, our results showed that *CgPOU2F1* and *CgSOX5* bound the promoter of the *CgHPX2*, and mutation of binding sites significantly decreased *CgHPX2* promoter activity, indicating two transcription factors positively regulate *CgHPX2*. What's more are the *CgPOU2F1* and *CgSOX5* subcellular localization in the nucleus. Therefore, we speculated that *CgPOU2F1* and *CgSOX5* may regulate the transcription of target genes in the nucleus. In addition, knockdown *CgPOU2F1* and *CgSOX5* led to a decrease in *CgHPX2* expression, suggesting that *CgPOU2F1* and *CgSOX5* can positively regulate *CgHPX2* expression. A decrease in *CgHPX2* expression implied that dsRNA-expression bacteria method applied in the larvae was reliable.

Conclusions

In summary, we identified and characterized *CgHPX2* gene from *C. gigas*. Temporal and spatial expression analysis of *CgHPX2* in different developmental stages and different tissues proved an important role in shell formation and pigmentation. Additionally, the core promoter region of the *CgHPX2* gene was found between −1519 and −1221 bp. The *CgPOU2F1* and *CgSOX5* were identified as the transcription factor motifs for *CgHPX2* transcription. Moreover, *CgPOU2F1* and *CgSOX5* were knocked down which can significantly downregulated the expression of *CgHPX2*. The findings presented here provided an insight into the basic transcriptional regulation mechanism of *CgHPX2* in shell pigmentation. This work would be valuable for further investigation on the pathway of melanin biosynthesis and shell formation in *C. gigas*.

Supplementary Information The online version contains supplementary material available at https://doi.org/10.1007/s10126-022-10098-z.

Funding This work was supported by the grants from National Natural Science Foundation of China (31972789), Earmarked Fund for Agriculture Seed Improvement Project of Shandong Province (2020LZGC016), China Agriculture Research System Project (CARS-49), Science and Technology Development Project of Weihai City (2018NS01), and Industrial Development Project of Qingdao City (20–3-4–16-nsh).

Declarations

Conflict of Interest The authors declare no competing interests.

References

Affenzeller S, Wolkenstein K, Frauendorf H, Jackson DJ (2019) Eumelanin and pheomelanin pigmentation in mollusc shells may be less common than expected: insights from mass spectrometry. Front Zool 16:47

Audino JA, Marian JEAR, Wanninger A, Lopes SGBC (2015) Mantle margin morphogenesis in *Nodipecten nodosus* (Mollusca: Bivalvia): new insights into the development and the roles of bivalve pallial folds. BMC Dev Biol 15:22

Besch R, Berking C (2014) POU transcription factors in melanocytes and melanoma. Eur J of Cell Biol 93:55–60

Boettiger A, Ermentrout B, Oster G (2009) The neural origins of shell structure and pattern in aquatic mollusks. Proc Natl Acad Sci U S A 106:6837–6842

Budd A, McDougall C, Green K, Degnan BM (2014) Control of shell pigmentation by secretory tubules in the abalone mantle. Front Zool 11:62

Charles D (2014) Cephalopod Ink: Production, Chemistry, Functions and Applications. Mar Drugs 12:2700–2730

Chen Y, Hu S, Mu L, Zhao B, Wang M, Yang N, Bao G, Zhu C, Wu X (2019) Slc7a11 modulated by POU2F1 is involved in pigmentation in rabbit. Int J Mol Sci 20:2493

Curran K, Raible DW, Lister JA (2009) Foxd3 controls melanophore specification in the zebrafish neural crest by regulation of Mitf. Dev Biol 332:408–417

Debbache J, Sommer L (2014) Sox5 and chromatophores: switching pigment cell fates. Pigm Cell Melanoma Res 27:1004–1013

Dondra B, Mohammed AB, Sanjay N, Nivedita B, Shaloei T, Duttaroy A (2017) The essential requirement of an animal heme peroxidase protein during the wing maturation process in Drosophila. BMC Dev Biol 17:1

Du J, Chen X, Wang J, Chen H, Yue W, Lu G, Wang C (2019) Comparative skin transcriptome of two Oujiang color common carp (*Cyprinus carpio var. color*) varieties. Fish Physiol Biochem 45:177–185

Feng D, Li Q, Yu H, Kong L, Du S (2017) Identification of conserved proteins from diverse shell matrix proteome in *Crassostrea gigas*: characterization of genetic bases regulating shell formation. Sci Rep 7:45754

Feng D, Li Q, Yu H (2019) RNA Interference by ingested dsRNA-expressing bacteria to study shell biosynthesis and pigmentation in *Crassostrea gigas*. Mar Biotechnol 21:526–536

Feng D, Li Q, Yu H, Liu S, Du S (2020) Integrated analysis of microRNA and mRNA expression profiles in *Crassostrea gigas* to reveal functional miRNA and miRNA-targets regulating shell pigmentation. Sci Rep 10:20238

Fowler DR, Meinhardt H, Prusinkiewicz P (1992) Modeling seashells. Comput Graph 26:379–387

Fujiwara H, Nishikawa H (2016) Functional analysis of genes involved in color pattern formation in Lepidoptera. Curr Opin Insect Sci 17:16–23

Ge JL, Li Q, Yu H, Kong LF (2015) Mendelian inheritance of golden shell color in the Pacific oyster *Crassostrea gigas*. Aquaculture 441:21–24

Gerhard H, Luitfried V, Salvini-Plawen RMR (1995) Larval planktotrophy—a primitive trait in the Bilateria? Acta Zool 76:141–154

Granger E, McNee G, Allan V, Woodman P (2014) The role of the cytoskeleton and molecular motors in endosomal dynamics. Semin Cell Dev Biol 31:20–29

Grant HE, Williams ST (2018) Phylogenetic distribution of shell colour in Bivalvia (Mollusca). Biol J Linn Soc 125:377–391

Han ZQ, Li Q (2020) Mendelian inheritance of orange shell color in the Pacific oyster *Crassostrea gigas*. Aquaculture 516.

Herlitze I, Marie B, Marin F, Jackson DJ (2018) Molecular modularity and asymmetry of the molluscan mantle revealed by a gene expression atlas. Gigascience 7

Hirosaki K, Yamashita T, Wada I, Jin HY, Jimbow K (2002) Tyrosinase and tyrosinase-related protein 1 require Rab7 for their intracellular transport. J Invest Dermatol 119:475–480

Hohagen J, Jackson DJ (2013) An ancient process in a modern mollusc: early development of the shell in *Lymnaea stagnalis*. BMC Dev Biol 13:27

Hohagen J, Herlitze I, Jackson DJ (2015) An optimised whole mount in situ hybridisation protocol for the mollusc *Lymnaea stagnalis*. BMC Dev Biol 15:19

Hu XW, Chen HL, Yu LW, Chen XW, Mandal BK, Wang J, Wang CH (2021) Functional differentiation analysis of duplicated mlpha gene in Oujiang color common carp (*Cyprinus carpio var. color*) on colour formation. Aquacult Res 52:4565–4573

Hu Z, Song H, Zhou C, Yu ZL, Yang MJ, Zhang T (2020) De novo assembly transcriptome analysis reveals the preliminary molecular mechanism of pigmentation in juveniles of the hard clam *Mercenaria mercenaria*. Genomics 112:3636–3647

Huan P, Wang HX, Liu BZ (2016) Assessment of housekeeping genes as internal references in quantitative expression analysis during early development of oyster. Genes Genet Syst 91:257–265

Huang S, Jiang H, Zhang L, Gu Q, Wang W, Wen Y, Luo F, Jin W, Cao X (2021) Integrated proteomic and transcriptomic analysis reveals that polymorphic shell colors vary with melanin synthesis in *Bellamya purificata* snail. J Proteomics 230:103950

Jackson DJ, Ellemor N, Degnan BM (2005) Correlating gene expression with larval competence, and the effect of age and parentage on metamorphosis in the tropical abalone *Haliotis asinina*. Mar Biol 147:681–697

Jackson DJ, Worheide G, Degnan BM (2007) Dynamic expression of ancient and novel molluscan shell genes during ecological transitions. BMC Evol Biol 7:160

Johnson AB, Fogel NS, Lambert JD (2019) Growth and morphogenesis of the gastropod shell. Proc Natl Acad Sci 116:6878–6883

Kang J, Shen Z, Lim JM, Handa H, Wells L, Tantin D (2013) Regulation of Oct1/Pou2f1 transcription activity by -GlcNAcylation. FASEB J 27:2807–2817

Kin K, Kakoi S, Wada H (2009) A novel role for dpp in the shaping of bivalve shells revealed in a conserved molluscan developmental program. Dev Biol 329:152–166

Kumar S, Stecher G, Tamura K (2016) MEGA7: molecular evolutionary genetics analysis version 7.0 for bigger datasets. Mol Biol Evol 33:1870–1874

Lemer S, Saulnier D, Gueguen Y, Planes S (2015) Identification of genes associated with shell color in the black-lipped pearl oyster. Pinctada Margaritifera BMC Genomics 16:568

Li H, Yu H, Li Q (2021) Striated myosin heavy chain gene is a crucial regulator of larval myogenesis in the pacific oyster *Crassostrea gigas*. Int J Biol Macromol 179:388–397

Loughran NB, O'Connor B, Ó'Fágáin C, O'Connell MJ (2008) The phylogeny of the mammalian heme peroxidases and the evolution of their diverse functions. BMC Evol Biol 8:101

Luo M, Lu G, Yin H, Wang L, Atuganile M, Dong Z (2021) Fish pigmentation and coloration: Molecular mechanisms and aquaculture perspectives. Rev Aquacult 13:2395–2412

Mao J, Zhang X, Zhang W, Tian Y, Wang X, Hao Z, Chang Y (2019) Genome-wide identification, characterization and expression analysis of the MITF gene in Yesso scallops (*Patinopecten yessoensis*) with different shell colors. Gene 688:155–162

Nagao Y, Takada H, Miyadai M, Adachi T, Seki R, Kamei Y, Hara I, Taniguchi Y, Naruse K, Hibi M, Kelsh RN, Hashimoto H (2018) Distinct interactions of Sox5 and Sox10 in fate specification of pigment cells in medaka and zebrafish. Plos Genet 14:e1007260

Nagao Y, Suzuki T, Shimizu A, Kimura T, Seki R, Adachi T, Inoue C, Omae Y, Kamei Y, Hara I, Taniguchi Y, Naruse K, Wakamatsu Y, Kelsh RN, Hibi M, Hashimoto H (2014) Sox5 functions as a fate switch in medaka pigment cell development. Plos Genet 10:e1004246

Nie H, Jiang K, Jiang L, Huo Z, Ding J, Yan X (2020) Transcriptome analysis reveals the pigmentation related genes in four different shell color strains of the Manila clam *Ruditapes philippinarum*. Genomics 112:2011–2020

Noh MY, Muthukrishnan S, Kramer KJ, Arakane Y (2016) Cuticle formation and pigmentation in beetles. Curr Opin Insect Sci 17:1–9

Ohbayashi N, Fukuda M (2020) Recent advances in understanding the molecular basis of melanogenesis in melanocytes. F1000Research 9:608

Parichy DM (2003) Pigment patterns: fish in stripes and spots. Curr Biol 13:R947–R950

Prud'homme B, Gompel N, Carroll SB (2007) Emerging principles of regulatory evolution. Proc Natl Acad Sci U S A 104:8605–8612

Rogers SL, Gelfand VI (2000) Membrane trafficking, organelle transport, and the cytoskeleton. Curr Opin Cell Biol 12:57–62

Shimizu K, Luo YJ, Satoh N, Endo K (2017) Possible co-option of engrailed during brachiopod and mollusc shell development. Biol Letters 13

Singh PK, Iqbal N, Sirohi HV, Bairagya HR, Singh TP (2017) Structural basis of activation of mammalian heme peroxidases. Prog Biophys Mol Biol 133:49–55

Sun X, Yang A, Wu B, Zhou L, Liu Z (2015) Characterization of the mantle transcriptome of Yesso scallop (*Patinopecten yessoensis*): identification of genes potentially involved in biomineralization and pigmentation. Plos One 10:el022967

Thompson CM, North EW, White SN, Gallager SM (2014) An analysis of bivalve larval shell pigments using micro-Raman spectroscopy. J Raman Spectrosc 45:349–358

Tian XY, Cui ZY, Liu S, Zhou J, Cui RT (2021) Melanosome transport and regulation in development and disease. Pharmacol Ther 219:107707

Timmermans L (1968) Studies On Shell Formation in Molluscs. Neth J Zool 19:413–523

Wang J, Zhang L, Lian S, Qin Z, Zhu X, Dai X, Huang Z, Ke C, Zhou Z, Wei J, Liu P, Hu N, Zeng Q, Dong B, Dong Y, Kong D, Zhang Z, Liu S, Xia Y, Li Y, Zhao L, Xing Q, Huang X, Hu X, Bao Z, Wang S (2020) Evolutionary transcriptomics of metazoan biphasic life cycle supports a single intercalation origin of metazoan larvae. Nat Ecol Evol 4:725–736

Wang P, Zhao Y, Fan R, Chen T, Dong C (2016) MicroRNA-21a-5p functions on the regulation of melanogenesis by targeting Sox5 in mouse skin melanocytes. Int J Mol Sci 17:959

Williams ST (2017) Molluscan shell colour. Biol Rev 92:1039–1058

Wittkopp PJ, Beldade P (2009) Development and evolution of insect pigmentation: Genetic mechanisms and the potential consequences of pleiotropy. Semin Cell Dev Biol 20:65–71

Xavier R, Patrice G (2014) Deciphering key features in protein structures with the new ENDscript server. Nucleic Acids Res 42:W320–W324

Xu C, Li Q, Yu H, Liu S, Kong L, Chong J (2019a) Inheritance of shell pigmentation in Pacific oyster *Crassostrea gigas*. Aquaculture 512:734249

Xu M, Huang J, Shi Y, Zhang H, He M (2019b) Comparative transcriptomic and proteomic analysis of yellow shell and black shell pearl oysters. Pinctada Fucata Martensii BMC Genomics 20:469

Yu F, Qu B, Lin D, Deng Y, Huang R, Zhong Z (2018) Pax3 gene regulated melanin synthesis by tyrosinase pathway in *Pteria penguin*. Int J Mol Sci 19

Yu J, Zhang L, Li Y, Li R, Zhang M, Li W, Xie X, Wang S, Hu X, Bao Z (2017) Genome-wide identification and expression profiling of the SOX gene family in a bivalve mollusc *Patinopecten yessoensis*. Gene 627:530–537

Yue C, Li Q, Yu H (2021) Variance in expression and localization of sex-related genes CgDsx, CgBHMG1 and CgFoxl2 during diploid and triploid Pacific oyster *Crassostrea gigas* gonad differentiation. Gene 790:145692

Zhang M, Chen X, Zhang J, Li J, Bai Z (2021) Cloning of a *HcCreb* gene and analysis of its effects on nacre color and melanin synthesis in *Hyriopsis cumingii*. PLoS One 16:e0251452

Zhang S, Wang H, Yu J, Jiang F, Yue X, Liu B (2018) Identification of a gene encoding microphthalmia-associated transcription factor and its association with shell color in the clam *Meretrix petechialis*. Comp. Biochem Physiol. Part b: Biochem Mol Biol 225:75–83

Zhu YJ, Li Q, Yu H, Liu SK, Kong LF (2021) Shell biosynthesis and pigmentation as revealed by the expression of tyrosinase and tyrosinase-like protein genes in Pacific oyster (*Crassostrea gigas*) with different shell colors. Mar Biotechnol